Coordinated Reconfigurable Intelligent Surfaces: Non-Diagonal Group-Connected Design

Qingchao Li, *Graduate Student Member, IEEE*,
Mohammed El-Hajjar, *Senior Member, IEEE*,
Ibrahim Hemadeh, *Member, IEEE*,
Arman Shojaeifard, *Senior Member, IEEE*,
Lajos Hanzo, *Life Fellow, IEEE*

***Abstract*—Reconfigurable intelligent surfaces (RIS) constitute a promising technology for future wireless communications in terms of improving the spectral-efficiency and energy-efficiency. In this context, a novel RIS structure, which we refer to as coordinated RIS architecture, is formulated, where different RIS elements can be connected by configurable impedances to eliminate the channel fading. In the proposed RIS architecture, both the RIS element connection pattern and the configurable impedances can be optimized, based on the channel state information (CSI). The proposed architecture exhibits higher optimization flexibility than the state-of-the-art single-connected RIS architecture and group-connected RIS architecture, where only the configurable impedances can be optimized. Specifically, when considering base stations (BS) having a single antenna, the maximal ratio combining (MRC) criterion may be harnessed for designing the RIS element connection pattern, while in the case of multiple BS antennas, the alternating optimization algorithm may be employed for iteratively optimizing the BS's active beamforming vector and the RIS's passive beamforming matrix. Our numerical results show that the proposed coordinated RIS architecture achieves higher power gain than the group-connected RIS architecture having the same number of configurable impedances. Furthermore, the power gain in our proposed RIS architecture tends to that of the fully-connected architecture upon increasing the number of RIS elements, while requiring significantly fewer configurable impedances.**

***Index Terms*—Reconfigurable intelligent surfaces (RIS), coordinated RIS, maximal ratio combining (MRC), alternating optimization.**

I. Introduction

One of the potential technologies designed for next generation wireless communications, namely reconfigurable intelligent surfaces (RIS), are constituted by software-controlled metasurface composed of a large number of passive reflecting elements which are capable of beneficially configuring the phase shift and amplitude of the impinging signals [1]. The employment of RISs has been shown to be beneficial in terms of extending the coverage to realize ubiquitous connection, combating channel fading, enhancing spectral efficiency, mitigating inter-user interference, etc [2].

In [3], Wu and Zhang formulated a joint beamforming scheme for RIS-assisted wireless systems, where the active beamforming at the base station (BS) and the passive beamforming at the RIS are jointly optimized for minimizing the transmit power subject to the received signal-to-interference-plus-noise ratio (SINR) constraints. For single-input-single-output (SISO) systems, the closed-form RIS beamforming matrix was mathematically derived, while for multiple-input-single-output (MISO) systems and multiple input multiple output (MIMO) systems, the alternating optimization and semidefinite relaxation (SDR) methods have been employed for finding the optimal or near-optimal solutions [3]. Furthermore, employing RISs has also been widely researched in a range of emerging areas, such as unmanned aerial vehicles (UAV) [4], Terahertz (THz) communications [5], integrated sensing and communications (ISAC) [6], etc.

The RIS elements in the above treatises are single-connected, where the signal impinging on a specific element can only be reflected from the same element after its phase/amplitude configuration. More specifically, there is no connection and coordination between different RIS elements, hence the potential of RIS is not fully exploited. In [7], Shen *et al.* proposed a novel RIS model, namely the group-connected RIS architecture, where the set of RIS elements is divided into multiple groups. In each group, the RIS elements are connected with each other, which means that the signal impinging on a specific element can be split and reflected from other elements in the same group. It was demonstrated that when the group size is the same as the total number of RIS elements, which was referred to as a fully-connected architecture, its power gain is $\frac{16}{\pi^2}$ times that of the single-connected RIS architecture under the Rayleigh fading channels in SISO systems. This was achieved at the cost of requiring more configurable impedances in the RIS circuits. In [8], Li *et al.* proposed a hybrid RIS architecture, where the RIS elements are placed on both sides of the plane to realize both reflection and refraction of the impinging signals. To achieve increased channel gain, the RIS elements are group-connected or fully-connected. In [9], this philosophy was extended to the multi-sector mode RIS architecture, where the RIS elements are spatially distributed on a polyhedron to realize three-dimension full-space coverage. In [10], we proposed a novel RIS architecture, where the incident signal impinging on a specific element can be reflected from another element according to a predefined routing, which is designed based on the channel state information (CSI) of the BS-RIS link and RIS-user link. It was shown that the power gain in our proposed RIS architecture is higher than that of the group-connected RIS architecture, and approaches that of the fully-connected RIS architecture, while requiring the same number of configurable impedances as the single-connected RIS architecture.

However, there are some limitations in the RIS architectures of [7], [8], [9], [10]. Firstly, in [7], [8], [9], the group partitioning is only based on the position indices of the RIS elements, which is not optimized based on the CSI. Secondly, in [10], the predefined routing is a one-to-one mapping. To deal with the above issues, our new contributions are as follows:

- We propose a novel structure, which we refer to as coordinated RIS architecture, where the signals impinging on specific elements can be reflected from other elements under some predefined routing. In contrast to [10], this routing is a group-to-group mapping, instead of being a one-to-one mapping. Therefore, a higher power gain can be achieved compared to the RIS architecture of [10]. Furthermore, the group-to-group mapping is optimized according to the CSI of the BS-RIS link and the RIS-user link, instead of solely optimizing the position indices of the RIS elements, which reveals that our proposed coordinated RIS architecture outperforms the group-connected RIS architecture of [7].
- The maximal ratio combining (MRC) criterion is employed to design the routing of group-to-group mapping, which exploits the CSI of the RIS-related links. Furthermore, we show how to jointly optimize the BS's active beamforming and the RIS's passive beamforming to maximize the power gain.
- The power gain of our proposed coordinated RIS architecture is verified by numerical simulations. We demonstrate that the coordinated RIS architecture achieves higher power gain than the group-connected RIS architecture having the same group size.

L. Hanzo would like to acknowledge the financial support of the Engineering and Physical Sciences Research Council projects EP/W016605/1, EP/X01228X/1, EP/Y026721/1 and EP/W032635/1 as well as of the European Research Council's Advanced Fellow Grant QuantCom (Grant No. 789028). *(Corresponding author: Lajos Hanzo.)*

Qingchao Li, Mohammed El-Hajjar and Lajos Hanzo are with the Electronics and Computer Science, University of Southampton, Southampton SO17 1BJ, U.K. (e-mail: qingchao.li@soton.ac.uk; meh@ecs.soton.ac.uk; lh@ecs.soton.ac.uk).

Ibrahim Hemadeh and Arman Shojaeifard are with InterDigital, London EC2A 3QR, U.K. (e-mail: ibrahim.hemadeh@interdigital.com; arman.shojaeifard@interdigital.com).

Furthermore, the power gain of our proposed coordinated RIS architecture tends to that of the fully-connected RIS architecture upon increasing the number of RIS elements, while requiring significantly fewer configurable impedances.

Notations: Vectors and matrices are denoted by boldface lower and upper case letters, respectively; $(\cdot)^{\mathrm{H}}$ represent the operation of Hermitian transpose; $\mathbb{C}^{m\times n}$ denotes the space of $m \times n$ complex-valued matrices; a_n represents the nth element of vector $\mathbf{a}$; $\mathbf{I}_N$ represents the $N \times N$ identity matrix; $\mathrm{diag}\{a_1, a_2, \cdots, a_N\}$ denotes a diagonal matrix with the diagonal elements being $a_1, a_2, \cdots, a_N$ in order; $\|\mathbf{x}\|$ and $\|\mathbf{X}\|$ represent the Euclidean norm of vector $\mathbf{x}$ and the Frobenius norm of matrix $\mathbf{X}$ respectively; $\mathcal{CN}(\boldsymbol{\mu}, \boldsymbol{\Sigma})$ is a circularly symmetric complex Gaussian random vector with the mean $\boldsymbol{\mu}$ and the covariance matrix $\boldsymbol{\Sigma}$; $[a_1; a_2; \cdots; a_N]$ represents an $N \times 1$ column vector while $[a_1, a_2, \cdots, a_N]$ represents a $1 \times N$ row vector.

II. System Model

Our RIS-aided wireless communication system model is shown in Fig. 1, which includes a base station (BS) having M antennas, a single-antenna user equipment (UE) and a RIS having N elements. We assume that the direct BS-UE link is blocked and only the RIS-aided two-hop link supports signal propagation. We denote the large scale fading of the BS-RIS link and the RIS-UE link as $\varrho_{\mathbf{h}}$ and $\varrho_{\mathbf{g}}$, respectively, and the small scale fading of the BS-RIS link and the RIS-UE link as $\mathbf{H} = [\mathbf{h}_1, \mathbf{h}_2, \cdots, \mathbf{h}_M] \in \mathbb{C}^{N\times M}$, and $\mathbf{g}^{\mathrm{H}} \in \mathbb{C}^{1\times N}$, respectively, where $\mathbf{h}_m \in \mathbb{C}^{N\times 1}$ denotes the CSI of the link spanning from the mth BS antenna to the RIS. We assume that the CSI, i.e. $\mathbf{H}$ and $\mathbf{g}^{\mathrm{H}}$, is known at the BS. In practice this is acquired by channel estimation [11]. Upon referring to [12], [13], we assume that both $\mathbf{h}_m$ and $\mathbf{g}$ obey Rician fading, given by

$$\mathbf{h}_m \sim \mathcal{CN}\Big(\sqrt{\frac{\kappa_{\mathbf{h}}}{1+\kappa_{\mathbf{h}}}}\overline{\mathbf{h}}_m, \sqrt{\frac{1}{1+\kappa_{\mathbf{h}}}}\mathbf{I}_N\Big), \tag{1}$$

$$\mathbf{g} \sim \mathcal{CN}\Big(\sqrt{\frac{\kappa_{\mathbf{g}}}{1+\kappa_{\mathbf{g}}}}\overline{\mathbf{g}}, \sqrt{\frac{1}{1+\kappa_{\mathbf{g}}}}\mathbf{I}_N\Big) \tag{2}$$

where $\overline{\mathbf{h}}_m$ and $\overline{\mathbf{g}}$ are the line-of-sight (LoS) components. We focus our attention on the downlink and denote the signal transmitted by the BS as $s \in \mathbb{C}^{1\times 1}$. Then, the signal received at the UE becomes:

$$r = \sqrt{\rho\varrho_{\mathbf{h}}\varrho_{\mathbf{g}}}\mathbf{g}^{\mathrm{H}}\boldsymbol{\Phi}\mathbf{H}\mathbf{v}s + w, \tag{3}$$

where ρ is the transmit power, $\mathbf{v}$ is the BS's active beamforming vector satisfying $\|\mathbf{v}\| = 1$, $w \sim \mathcal{CN}(0, \sigma_w^2)$ is the additive noise at the UE, and $\boldsymbol{\Phi}$ denotes the RIS's passive beamforming matrix. We define the *power gain* at the receiver due to the RIS as [7]

$$\mathcal{G} = \|\mathbf{g}^{\mathrm{H}}\boldsymbol{\Phi}\mathbf{H}\mathbf{v}\|^2. \tag{4}$$

In the following, firstly the state-of-the-art diagonal single-connected RIS architecture and block-diagonal group-connected RIS architecture are presented. Then, we introduce our proposed non-diagonal coordinated RIS architecture.

A. Conventional single-connected RIS architecture

Again, in the conventional single-connected RIS architecture, the signal impinging on the nth element only can be reflected from the nth element [3]–[6], [14]. Therefore, the RIS's beamforming matrix $\boldsymbol{\Phi}$ is diagonal, given by

$$\boldsymbol{\Phi} = \mathrm{diag}\left\{\phi_{1,1}, \phi_{2,2}, \cdots, \phi_{N,N}\right\}. \tag{5}$$

Since the RIS is passive without power amplification, it satisfies the constraint that $\|\phi_{n,n}\|^2 = 1$ for $n = 1, 2, \cdots, N$. For example,

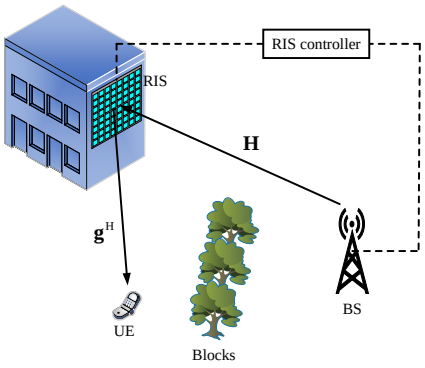

Fig. 1: System model of the considered RIS-aided wireless communication system.

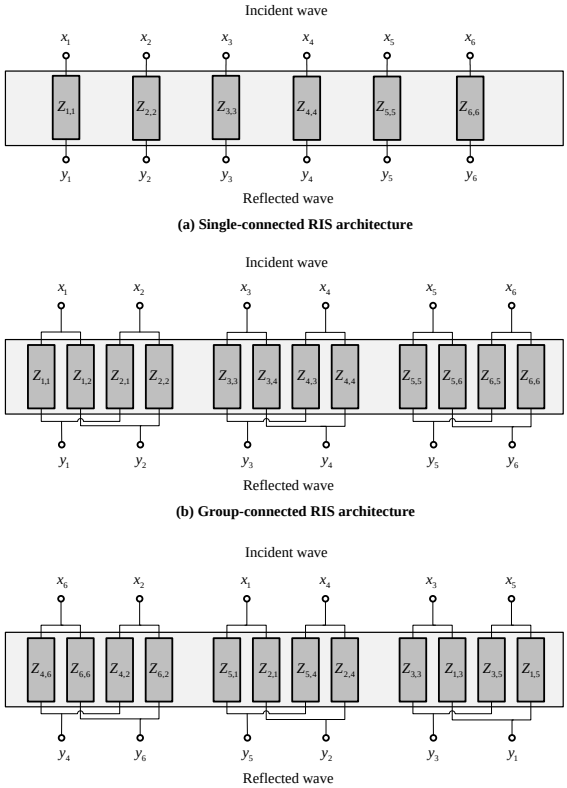

Fig. 2: An example of the transmission line model of (a) the single-connect RIS architecture, (b) the group-connected RIS architecture, and (c) the coordinated RIS architecture.

when $N = 6$, the classic transmission line model [15] of the single-connected RIS architecture is shown in Fig. 2 (a), where x_n and y_n represent the incident signal and the reflected signal at the nth RIS element, respectively. Furthermore, $Z_{n,n}$ is the configurable impedance in the nth RIS element, given by $Z_{n,n} = \frac{1+\phi_{n,n}}{1-\phi_{n,n}}Z_0$, where Z_0 is the free-space impedance [7].

B. Group-connected RIS architecture

Since the RIS elements of the conventional RIS architecture are single-connected, it cannot achieve the full potential in combating the channel fading [7]. If there is a connection between different RIS elements, where the incident signal impinging on the nth element can be reflected from other elements, then it will facilitate flexible RIS phase shift matrix designs, which can improve the attainable channel

gain. To achieve this goal, the group-connected RIS architecture was proposed in [7], where the N RIS elements are partitioned into $\frac{N}{G}$ groups, with each group having G elements. In each group, the G elements are connected to each other by configurable impedances. Thus, the RIS's beamforming matrix is block diagonal, given by

$$\mathbf{\Phi} = \text{diag}\{\mathbf{\Phi}_1, \mathbf{\Phi}_2, \cdots, \mathbf{\Phi}_{\frac{N}{G}}\}, \tag{6}$$

where $\mathbf{\Phi}_i$ $(i = 1, 2, \cdots, \frac{N}{G})$ represents the RIS phase shift matrix of the ith group. For example, the transmission line model of the group-connected RIS architecture with $N = 6$ and $G = 2$ is shown in Fig. 2 (b) and the corresponding RIS phase shift matrix is

$$\mathbf{\Phi} = \text{diag}\{\mathbf{\Phi}_1, \mathbf{\Phi}_2, \mathbf{\Phi}_3\}, \tag{7}$$

where $\mathbf{\Phi}_1 = \begin{bmatrix} \phi_{1,1} & \phi_{1,2} \\ \phi_{2,1} & \phi_{2,2} \end{bmatrix}$, $\mathbf{\Phi}_2 = \begin{bmatrix} \phi_{3,3} & \phi_{3,4} \\ \phi_{4,3} & \phi_{4,4} \end{bmatrix}$ and $\mathbf{\Phi}_3 = \begin{bmatrix} \phi_{5,5} & \phi_{5,6} \\ \phi_{6,5} & \phi_{6,6} \end{bmatrix}$. Furthermore, Z_{n_1,n_2} is the configurable impedance for the wave incident on the n_2th RIS element and reflected from the n_1th RIS elements, as shown in Fig. 2 (b), given by $Z_{n_1,n_2} = \frac{1+\phi_{n_1,n_2}}{1-\phi_{n_1,n_2}} Z_0$.

Since the RIS is passive, we have to satisfy $\|\mathbf{\Phi}_i\|^2 = 1$ for $i = 1, 2, \cdots, \frac{N}{G}$. In the single-connected RIS architecture there are only N configurable impedances, while in the group-connected RIS architecture there are GN configurable impedances, hance improved configuration flexility can be achieved in the group-connected RIS to achieve high power gain. As a special case, when $G = N$, there will be N^2 configurable impedances and the RIS architecture becomes fully-connected.

C. The proposed coordinated RIS architecture

Although the group-connected RIS architecture achieves increased power gain by employing more configurable impedances to connect the different RIS elements, it still cannot achieve the full potential of RIS, because the RIS elements are grouped by their natural indices instead of based on the CSI of $\mathbf{H}$ and $\mathbf{g}^{\text{H}}$. For example, in Fig. 2 (b), the incident waves (x_1, x_2), (x_3, x_4) and (x_5, x_6) are assigned into three different groups, and the reflected waves (y_1, y_2), (y_3, y_4) and (y_5, y_6) are assigned into three different groups. Then, we can characterize this element connection mapping as

$$\mathcal{M}: \begin{array}{c} \{x_1, x_2\} \to \{y_1, y_2\} \\ \{x_3, x_4\} \to \{y_3, y_4\} \\ \{x_5, x_6\} \to \{y_5, y_6\} \end{array}. \tag{8}$$

Since the element connection mapping is fixed in the group-connected RIS architecture, it may not be optimal. On the other hand, the power gain can be further improved if we can optimize the element connection pattern. Therefore, we propose the coordinated RIS architecture, where not only the impedances can be configured, but also the element connection pattern can be optimized based on the CSI realization encountered, which can bring about improved configurable flexibility to achieve increased power gain. In the practical hardware circuit, a potential implementation of the group mapping can be realized by switch arrays using RF micro-electronmechanical systems (MEMS) [10].

For example, when $N = 6$ and $G = 2$, we assume that the optimal elements connection mapping in a specific CSI realization is

$$\mathcal{M}: \begin{array}{c} \{x_6, x_2\} \to \{y_4, y_6\} \\ \{x_1, x_4\} \to \{y_5, y_2\} \\ \{x_3, x_5\} \to \{y_3, y_1\} \end{array}. \tag{9}$$

Note that this mapping is just shown as an example and the real selected optimal elements connection mapping based on the CSI realization will be discussed in the next section. Then the transmission line model of the RIS architecture is given in Fig. 2 (c) and the corresponding RIS's beamforming matrix is given by

$$\mathbf{\Phi} = \begin{bmatrix} 0 & 0 & \phi_{1,3} & 0 & \phi_{1,5} & 0 \\ \phi_{2,1} & 0 & 0 & \phi_{2,4} & 0 & 0 \\ 0 & 0 & \phi_{3,3} & 0 & \phi_{3,5} & 0 \\ 0 & \phi_{4,2} & 0 & 0 & 0 & \phi_{4,6} \\ \phi_{5,1} & 0 & 0 & \phi_{5,4} & 0 & 0 \\ 0 & \phi_{6,2} & 0 & 0 & 0 & \phi_{6,6} \end{bmatrix} = \mathbf{J}_r \widetilde{\mathbf{\Phi}} \mathbf{J}_c, \tag{10}$$

where $\widetilde{\mathbf{\Phi}} = \text{diag}\{\widetilde{\mathbf{\Phi}}_1, \widetilde{\mathbf{\Phi}}_2, \widetilde{\mathbf{\Phi}}_3\}$ with $\widetilde{\mathbf{\Phi}}_1 = \begin{bmatrix} \phi_{4,6} & \phi_{4,2} \\ \phi_{6,6} & \phi_{6,2} \end{bmatrix}$, $\widetilde{\mathbf{\Phi}}_2 = \begin{bmatrix} \phi_{5,1} & \phi_{5,4} \\ \phi_{2,1} & \phi_{2,4} \end{bmatrix}$, and $\widetilde{\mathbf{\Phi}}_3 = \begin{bmatrix} \phi_{3,3} & \phi_{3,5} \\ \phi_{1,3} & \phi_{1,5} \end{bmatrix}$. $\mathbf{J}_r = [\mathbf{e}_4, \mathbf{e}_6, \mathbf{e}_5, \mathbf{e}_2, \mathbf{e}_3, \mathbf{e}_1]$ and $\mathbf{J}_c = [\mathbf{e}_6, \mathbf{e}_2, \mathbf{e}_1, \mathbf{e}_4, \mathbf{e}_3, \mathbf{e}_5]^{\text{H}}$ are row permutation matrix and column matrix, respectively, in which $\mathbf{e}_n$ is an $N \times 1$ vector with the nth element being 1 and other elements being 0. In the group-connected RIS architecture, the permutation matrices $\mathbf{J}_r$ and $\mathbf{J}_c$ are fixed as $\mathbf{I}_N$, while in our proposed coordinated RIS architecture, the permutation matrices $\mathbf{J}_r$ and $\mathbf{J}_c$ can be optimized based on the CSI realization.

Since the RIS is passive, we need to satisfy $\|\mathbf{\Phi}_i\|^2 = 1$ for $i = 1, 2, \cdots, \frac{N}{G}$ in our proposed coordinated RIS architecture. In Fig. 2 (c), we can find that the number of impedances is the same as that of the group-connected RIS architecture in Fig. 2 (b). However, the element connection mapping in our proposed coordinated RIS architecture can be optimized, which is promising to provide higher power gain.

III. Beamforming Design

In this section, we present the design of active beamforming $\mathbf{v}$ at the BS and the passive RIS phase shift matrix $\mathbf{\Phi}$ at the RIS based on the CSI.

A. Single BS Antenna

When the BS has a single antenna, i.e. $M = 1$, the BS-RIS channel matrix $\mathbf{H} \in \mathbb{C}^{N \times M}$ is degenerated to the vector $\mathbf{h} \in \mathbb{C}^{N \times 1}$, and the BS's beamforming vector is fixed as $\mathbf{v} = 1$. In this case, the received signal at the UE in (3) will be

$$r = \sqrt{\rho \varrho_{\mathbf{h}} \varrho_{\mathbf{g}}} \mathbf{g}^{\text{H}} \mathbf{\Phi} \mathbf{h} s + w, \tag{11}$$

and power gain in (4) will be

$$\mathcal{G} = \|\mathbf{g}^{\text{H}} \mathbf{\Phi} \mathbf{h}\|^2. \tag{12}$$

Here, our purpose is to design the RIS's beamforming matrix $\mathbf{\Phi}$ to maximize the power gain in (12).

1) Conventional single-connected RIS architecture: In the conventional single-connected RIS architecture, the optimal $\phi_{n,n}$ in the RIS's beamforming matrix in (5) can be obtained as [2]

$$\phi_{n,n} = \frac{g_n}{\|g_n\|} \frac{h_n^{\text{H}}}{\|h_n\|}. \tag{13}$$

2) Group-connected RIS architecture: We denote the elements in the channel vector $\mathbf{h}$ corresponding to the ith group as $\mathbf{h}_i$, and the elements in the channel vector $\mathbf{g}^{\text{H}}$ corresponding to the ith group as $\mathbf{g}_i^{\text{H}}$. For example, in (7), $\mathbf{h}_1 = [h_1; h_2]$, $\mathbf{h}_2 = [h_3; h_4]$, $\mathbf{h}_3 = [h_5; h_6]$, and $\mathbf{g}_1^{\text{H}} = [g_1^{\text{H}}, g_2^{\text{H}}]$, $\mathbf{g}_2^{\text{H}} = [g_3^{\text{H}}, g_4^{\text{H}}]$, $\mathbf{g}_3^{\text{H}} = [g_5^{\text{H}}, g_6^{\text{H}}]$. In this case, the power gain becomes

$$\mathcal{G} = \sum_{i=1}^{\frac{N}{G}} \|\mathbf{g}_i^{\text{H}} \mathbf{\Phi}_i \mathbf{h}_i\|^2. \tag{14}$$

According to the Cauchy-Schwarz inequality, we can get

$$\|\mathbf{g}_i^{\mathrm{H}}\mathbf{\Phi}_i\mathbf{h}_i\| \leq \|\mathbf{g}_i^{\mathrm{H}}\mathbf{\Phi}_i\| \cdot \|\mathbf{h}_i\|, \tag{15}$$

where the equality is established only when $\mathbf{g}_i^{\mathrm{H}}\mathbf{\Phi}_i = \alpha\mathbf{h}_i$, where $\alpha \neq 0$. Since $\|\mathbf{\Phi}_i\|^2 = 1$, the optimal $\mathbf{\Phi}_i$ can be obtained as [7]

$$\mathbf{\Phi}_i = \frac{\mathbf{g}_i}{\|\mathbf{g}_i\|}\frac{\mathbf{h}_i^{\mathrm{H}}}{\|\mathbf{h}_i\|}. \tag{16}$$

3) The proposed coordinated RIS architecture: In our proposed coordinated RIS architecture, firstly we have to select the optimal element connection pattern $\mathcal{M}$, i.e. the row permutation matrix $\mathbf{J}_r$ and the column permutation matrix $\mathbf{J}_c$. Then, based on the selected element connection pattern $\mathcal{M}$, we optimize the configurable impedances, which corresponds to the block diagonal matrix $\widetilde{\mathbf{\Phi}}$.

Firstly, according to the MRC criterion, the power gain can be maximized when the mapping between the incident wave and the reflected wave is designed based on the amplitude order in the vector $\mathbf{h}$ and $\mathbf{g}$. Specifically, we denote $\widetilde{\mathbf{h}}$ as the vector $\mathbf{h}$ sorted in a descending order, given by $\widetilde{\mathbf{h}} = [h_{(1)}; h_{(2)}; \cdots; h_{(N)}]$, where $h_{(n)}$ is the element in vector $\mathbf{h}$ with the nth largest amplitude, and we formulate the index vector $\mathbf{p}$ as $\mathbf{p} = [p_1; p_2; \cdots; p_N]$, where p_n is the index of element $h_{(n)}$ in the vector $\mathbf{h}$. Similarly, we denote $\widetilde{\mathbf{g}}$ as the descending-order-sorted vector of $\mathbf{g}$, given by $\widetilde{\mathbf{g}} = [g_{(1)}; g_{(2)}; \cdots; g_{(N)}]$ and denote the index vector $\mathbf{q}$ as $\mathbf{q} = [q_1; q_2; \cdots; q_N]$ where q_n is the index of element $g_{(n)}$ in the vector $\mathbf{g}$. Based on the MRC criterion, the element connection mapping obeys

$$\mathcal{M}: \begin{array}{c} \{x_{p_1}, \cdots, x_{p_G}\} \to \{y_{q_1}, \cdots, y_{q_G}\} \\ \{x_{p_{G+1}}, \cdots, x_{p_{2G}}\} \to \{y_{q_{G+1}}, \cdots, y_{q_{2G}}\} \\ \vdots \\ \{x_{p_{N-G+1}}, \cdots, x_{p_N}\} \to \{y_{q_{N-G+1}}, \cdots, y_{q_N}\} \end{array}. \tag{17}$$

Based on the group mapping $\mathcal{M}$, the corresponding row permutation matrix and column permutation matrix are given by $\mathbf{J}_r = [\mathbf{e}_{q_1}, \mathbf{e}_{q_2}, \cdots, \mathbf{e}_{q_N}]$ and $\mathbf{J}_c = [\mathbf{e}_{p_1}, \mathbf{e}_{p_2}, \cdots, \mathbf{e}_{p_N}]^{\mathrm{H}}$, respectively.

Once the row permutation matrix and column permutation matrix are determined, the bock diagonal matrix $\widetilde{\mathbf{\Phi}} = \mathrm{diag}\{\widetilde{\mathbf{\Phi}}_1, \widetilde{\mathbf{\Phi}}_2, \cdots, \widetilde{\mathbf{\Phi}}_{\frac{N}{G}}\}$ can be designed similar to the case of the group-connected RIS architecture. Specifically, $\widetilde{\mathbf{\Phi}}_i$ is given by

$$\begin{aligned}\widetilde{\mathbf{\Phi}}_i &= \begin{bmatrix} \phi_{q_{(i-1)G+1},p_{(i-1)G+1}} & \cdots & \phi_{q_{(i-1)G+1},p_{iG}} \\ \vdots & \ddots & \vdots \\ \phi_{q_{iG},p_{(i-1)G+1}} & \cdots & \phi_{q_{iG},p_{iG}} \end{bmatrix} \\ &= \frac{\widetilde{\mathbf{g}}_i}{\|\widetilde{\mathbf{g}}_i\|}\frac{\widetilde{\mathbf{h}}_i^{\mathrm{H}}}{\|\widetilde{\mathbf{h}}_i\|},\end{aligned} \tag{18}$$

where $\widetilde{\mathbf{h}}_i = [\widetilde{h}_{(i-1)G+1}; \cdots; \widetilde{h}_{iG}] = [h_{(p_{(i-1)G+1})}; \cdots; h_{(p_{iG})}]$ and $\widetilde{\mathbf{g}}_i = [\widetilde{g}_{(i-1)G+1}; \cdots; \widetilde{g}_{iG}] = [g_{(q_{(i-1)G+1})}; \cdots; g_{(q_{iG})}]$. Then, the final RIS's beamforming matrix $\mathbf{\Phi}$ of our proposed coordinated RIS architecture is given by

$$\begin{aligned}\mathbf{\Phi} =& [\mathbf{e}_{q_1}, \cdots, \mathbf{e}_{q_N}] \cdot \mathrm{diag}\Big\{\frac{\widetilde{\mathbf{g}}_1}{\|\widetilde{\mathbf{g}}_1\|}\frac{\widetilde{\mathbf{h}}_1^{\mathrm{H}}}{\|\widetilde{\mathbf{h}}_1\|}, \cdots, \frac{\widetilde{\mathbf{g}}_{\frac{N}{G}}}{\|\widetilde{\mathbf{g}}_{\frac{N}{G}}\|}\frac{\widetilde{\mathbf{h}}_{\frac{N}{G}}^{\mathrm{H}}}{\|\widetilde{\mathbf{h}}_{\frac{N}{G}}\|}\Big\} \cdot \\ & \Big[\mathbf{e}_{p_1}^{\mathrm{H}}; \cdots; \mathbf{e}_{p_N}^{\mathrm{H}}\Big].\end{aligned} \tag{19}$$

Theorem 1. Based on the MRC criterion, the power gain can be maximized when the group mapping obeys the relationship in (17).

Proof: Based on the element connection mapping of (17) and the RIS's beamforming matrix $\mathbf{\Phi}$ in (19), the power gain can be expressed as

$$\mathcal{G} = \sum_{i=1}^{\frac{N}{G}} \|\widetilde{\mathbf{g}}_i^{\mathrm{H}}\widetilde{\mathbf{\Phi}}_i\widetilde{\mathbf{h}}_i\|^2 = \sum_{i=1}^{\frac{N}{G}} \|\widetilde{\mathbf{g}}_i\|^2\|\widetilde{\mathbf{h}}_i\|^2. \tag{20}$$

If we arbitrarily pick out two entries $x_{p_{(t_1-1)G+g_1}}$ and $x_{p_{(t_2-1)G+g_2}}$ and swap them in (17) with $t_1 < t_2$, a new group mapping will be constructed. Let us denote the corresponding power gain as $\mathcal{G}'$. Therefore, we can get

$$\begin{aligned}\mathcal{G} - \mathcal{G}' =& (\|\widetilde{\mathbf{g}}_{t_1}\|^2\|\widetilde{\mathbf{h}}_{t_1}\|^2 + \|\widetilde{\mathbf{g}}_{t_2}\|^2\|\widetilde{\mathbf{h}}_{t_2}\|^2) \\ & - (\|\widetilde{\mathbf{g}}_{t_1}\|^2\|\widetilde{\mathbf{h}}'_{t_1}\|^2 + \|\widetilde{\mathbf{g}}_{t_2}\|^2\|\widetilde{\mathbf{h}}'_{t_2}\|^2),\end{aligned} \tag{21}$$

where $\widetilde{\mathbf{h}}'_{t_1} = [\widetilde{h}_{(t_1-1)G+1}; \cdots; \widetilde{h}_{(t_1-1)G+g_1-1}; \widetilde{h}_{(t_2-1)G+g_2}; \widetilde{h}_{(t_1-1)G+g_1+1}; \cdots; \widetilde{h}_{t_1G}]$, and $\widetilde{\mathbf{h}}'_{t_2} = [\widetilde{h}_{(t_2-1)G+1}; \cdots; \widetilde{h}_{(t_2-1)G+g_2-1}; \widetilde{h}_{(t_1-1)G+g_1}; \widetilde{h}_{(t_2-1)G+g_2+1}; \cdots; \widetilde{h}_{t_2G}]$. Then, $\mathcal{G} - \mathcal{G}'$ in (20) can be further reformulated as

$$\begin{aligned}\mathcal{G} - \mathcal{G}' =& (|\widetilde{h}_{(t_1-1)G+g_1}|^2 - |\widetilde{h}_{(t_2-1)G+g_2}|^2)(\|\widetilde{\mathbf{g}}_{t_1}\|^2 - \|\widetilde{\mathbf{g}}_{t_2}\|^2) \\ \overset{(a)}{\geq}& 0,\end{aligned} \tag{22}$$

where (a) is based on $|\widetilde{h}_{(t_1-1)G+g_1}| \geq |\widetilde{h}_{(t_2-1)G+g_2}|$ and $\|\widetilde{\mathbf{g}}_{t_1}\| \geq \|\widetilde{\mathbf{g}}_{t_2}\|$ since $t_1 < t_2$. Thus, the power gain can be maximized when the group mapping is designed based on the MRC criterion in (17). ■

Algorithm 1 Alternating optimization algorithm for joint beamforming of MISO systems with the coordinated RIS architecture.

Input: The BS-RIS channel $\mathbf{H}$, the RIS-UE channel $\mathbf{g}^{\mathrm{H}}$, and the group size G.

Get the descending-sorted vector $\widetilde{\mathbf{g}}^{\mathrm{H}}$ based on $\mathbf{g}^{\mathrm{H}}$, and derive the corresponding row permutation matrix $\mathbf{J}_r$ satisfying $\mathbf{g}^{\mathrm{H}} = \widetilde{\mathbf{g}}^{\mathrm{H}}\mathbf{J}_r$.
Set the random initial BS's beamforming vector $\mathbf{v}$ satisfying $\|\mathbf{v}\| = 1$.
for $i = 1$ **to** $\frac{N}{G}$
    $\widetilde{\mathbf{g}}_i = \big[\widetilde{g}_{(i-1)G+1}; \widetilde{g}_{(i-1)G+2}; \cdots; \widetilde{g}_{iG}\big]$.
end
Repeat
    The equivalent BS-RIS channel $\mathbf{h} = \mathbf{H}\mathbf{v}$.
    Get the descending-sorted vector $\widetilde{\mathbf{h}}$ based on $\mathbf{h}$, and derive the corresponding permutation matrix $\mathbf{J}_r$ satisfying $\mathbf{h} = \mathbf{J}_r\widetilde{\mathbf{h}}$.
    for $i = 1$ **to** $\frac{N}{G}$
        $\widetilde{\mathbf{h}}_i = [\widetilde{h}_{(i-1)G+1}; \widetilde{h}_{(i-1)G+2}; \cdots; \widetilde{h}_{iG}]$.
        $\widetilde{\mathbf{\Phi}}_i = \frac{\widetilde{\mathbf{g}}_i}{\|\widetilde{\mathbf{g}}_i\|}\frac{\widetilde{\mathbf{h}}_i^{\mathrm{H}}}{\|\widetilde{\mathbf{h}}_i\|}$.
    end
    $\widetilde{\mathbf{\Phi}} = \mathrm{diag}\{\widetilde{\mathbf{\Phi}}_1, \widetilde{\mathbf{\Phi}}_2, \cdots, \widetilde{\mathbf{\Phi}}_{\frac{N}{G}}\}$.
    The RIS's beamforming matrix $\mathbf{\Phi} = \mathbf{J}_r\widetilde{\mathbf{\Phi}}\mathbf{J}_c$.
    The BS's beamforming $\mathbf{v} = \frac{(\mathbf{g}^{\mathrm{H}}\mathbf{\Phi}\mathbf{H})^{\mathrm{H}}}{\|\mathbf{g}^{\mathrm{H}}\mathbf{\Phi}\mathbf{H}\|}$.
Until reaching the iteration times.

Output: The optimized BS's beamforming vector $\mathbf{v}$, and the optimized RIS's beamforming matrix $\mathbf{\Phi}$.

B. Multiple BS Antennas

When the number of BS antennas is $M > 1$, the BS' active beamforming vector $\mathbf{v}$ and the RIS's passive beamforming matrix $\mathbf{\Phi}$ should be jointly optimized for maximizing the power gain. The objective function can be formulated as

$$\begin{aligned}\text{(P1)} \quad & \max_{\mathbf{v},\mathbf{\Phi}} \ \|\mathbf{g}^{\mathrm{H}}\mathbf{\Phi}\mathbf{H}\mathbf{v}\|^2 \\ & \text{s.t.} \quad \|\mathbf{v}\| = 1,\end{aligned}$$

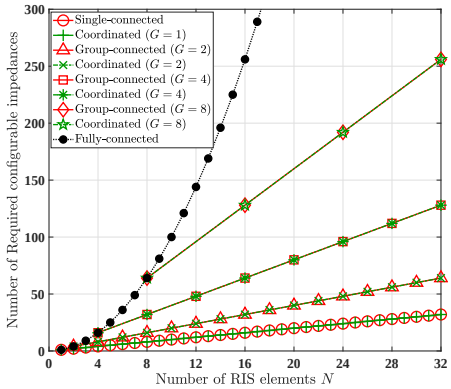

Fig. 3: Comparison of the number of required configurable impedances versus the number of RIS elements N for different RIS architectures.

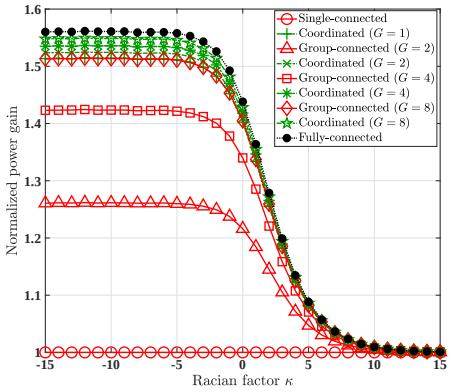

Fig. 4: Comparison of the normalized power gain versus the Rician factor κ for different RIS architectures.

$$\mathbf{\Phi} = \mathbf{J}_r \widetilde{\mathbf{\Phi}} \mathbf{J}_c, \quad \widetilde{\mathbf{\Phi}} = \text{diag}\{\widetilde{\mathbf{\Phi}}_1, \widetilde{\mathbf{\Phi}}_2, \cdots, \widetilde{\mathbf{\Phi}}_{\frac{N}{G}}\},$$
$$\|\widetilde{\mathbf{\Phi}}_i\|^2 = 1, \quad i = 1, 2, \cdots, \frac{N}{G}. \tag{23}$$

The problem (P1) can be solved by applying alternating optimization method. Specifically, in each iteration, when the RIS's beamforming matrix $\mathbf{\Phi}$ is given, the equivalent channel of the RIS-aided system is $\mathbf{g}^{\mathrm{H}}\mathbf{\Phi}\mathbf{H}$. Then, the BS's beamforming can be optimized by the MRC method, designed as $\mathbf{v} = \frac{\left(\mathbf{g}^{\mathrm{H}}\mathbf{\Phi}\mathbf{H}\right)^{\mathrm{H}}}{\|\mathbf{g}^{\mathrm{H}}\mathbf{\Phi}\mathbf{H}\|}$ for maximizing the power gain [3]. By contrast, when the BS's beamforming vector $\mathbf{v}$ is given, the equivalent channel link spanning form the BS to the RIS is given by $\mathbf{h} = \mathbf{H}\mathbf{v}$, and then the RIS's beamforming matrix can be optimized in a similar way to the case of a single BS antenna. The detailed process of the alternating optimization algorithm of the joint beamforming design conceived for the proposed coordinated RIS-aided MISO system is shown in Algorithm 1.

IV. Simulation Results and Analysis

Firstly, we compare the hardware implementation complexity of different RIS architectures. Fig. 3 compares the number of required configurable impedances versus the number of RIS elements N for different RIS architectures, including our proposed coordinated RIS architecture, the conventional single-connected RIS architecture, as well as the fully-connected RIS architecture and the group-connected RIS of [7]. Fig. 3 shows the number of configurable impedances required by the single-connected RIS architecture, the group-connected RIS architecture and our proposed coordinated RIS architecture, which is considerably lower than that of the fully-connected RIS architecture. When the group size is $G = 1$, the number of configurable impedances required for the proposed design is the same as that of the single-connected RIS architecture. When the group size is $G > 1$, the number of configurable impedances required is the same as that of the group-connected RIS architecture at the same value of G.

When the number of BS antennas is $M = 1$, in Fig. 4 we compare the power gain of different RIS architectures, normalized by that in the single-connected RIS architecture, versus the Rician factors, where we have $\kappa = \kappa_{\mathbf{g}} = \kappa_{\mathbf{h}}$ and the number of RIS

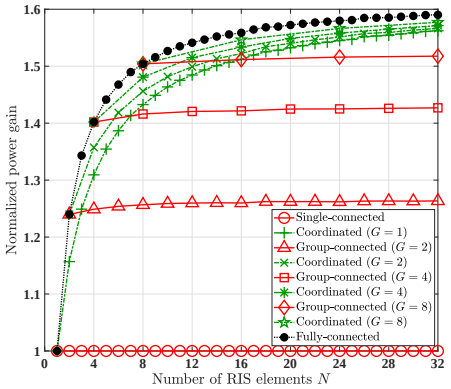

Fig. 5: Comparison of the normalized power gain versus the number of RIS elements N for different RIS architectures.

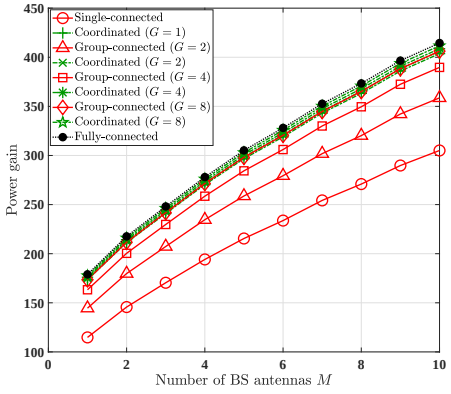

(a) $N = 16$

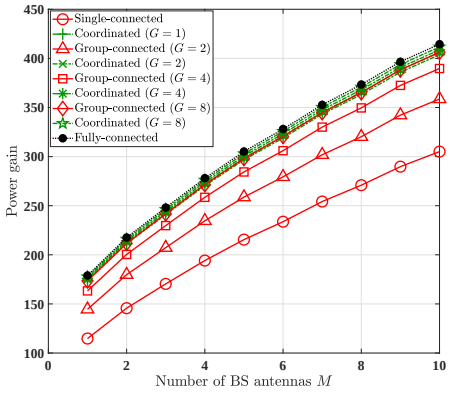

(b) $N = 32$

Fig. 6: Comparison of the power gain versus the number of BS antennas M for different RIS architectures, with different numbers of RIS elements.

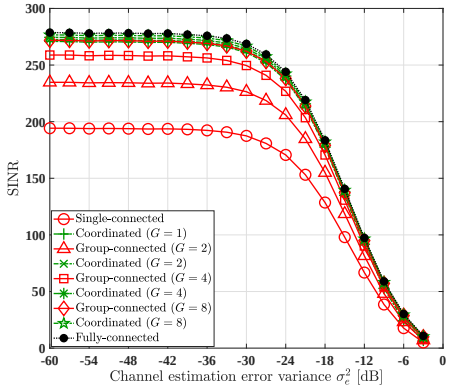

Fig. 7: Comparison of the SINR versus channel estimation error variance σ_e^2 for different RIS architectures.

elements is $N = 16$. The figure shows that the group/fully-connected RIS architecture and our proposed coordinated RIS architecture outperform the conventional diagonal RIS architecture in the low Rician factor region. Furthermore, it also shows that our proposed coordinated RIS architecture achieves higher power gain than the conventional group-connected RIS architecture.

Then, the power gain of different RIS architectures in the Rayleigh fading channel with single BS antenna, normalized by that in the single-connected RIS architecture, versus the number of RIS elements N is shown in Fig. 5. Observe from Fig. 5 the clear performance gap between the group-connected RIS architecture and the fully-connected RIS architecture. By contrast, the power gain in our proposed coordinated RIS architecture is constantly higher than that of the group-connected RIS architecture having the same group size G. The group-connected RIS architecture has a fixed element connection pattern, while in our proposed coordinated RIS architecture, the element connection pattern can be optimized based on the CSI for further increasing the power gain. Furthermore, upon increasing of the number of RIS elements N, the power gain of our proposed coordinated RIS architecture tends to that of the fully-connected RIS architecture, while requiring considerably fewer configurable impedances.

Fig. 6 compares the power gain versus the number of BS antennas M for different RIS architectures, with different number of RIS elements, where the Rician factor $\kappa_{\mathbf{h}} = \kappa_{\mathbf{g}} = -10\text{dB}$. Fig. 6 shows that the power gain increases almost linearly with the number of BS antennas. When the number of RIS elements is $N = 16$, our proposed coordinated RIS architecture having $G = 2$ achieves almost the same power gain as the group-connected RIS architecture having $G = 8$. Furthermore, when the number of RIS elements is $N = 32$, the power gain in our proposed coordinated RIS architecture is higher than that of the group-connected RIS architecture and tightly tends to that of the fully-connected RIS architecture.

When considering imperfect CSI, referring to [16], the BS-RIS link and the RIS-UE link can be represented as $\mathbf{H} = \hat{\mathbf{H}} + \mathbf{H}_e$ and $\mathbf{g}^{\mathrm{H}} = \hat{\mathbf{g}}^{\mathrm{H}} + \mathbf{g}_e^{\mathrm{H}}$, where $\hat{\mathbf{H}}$ and $\hat{\mathbf{g}}^{\mathrm{H}}$ are the estimated channel links, while $\mathbf{H}_e$ and $\mathbf{g}_e^{\mathrm{H}}$ represents the CSI estimation error component, where each entry obeys $\mathcal{CN}(0, \sigma_e^2)$. Fig. 7 represents the resulting SINR given the error variance σ_e^2 for different RIS architectures, where $\frac{\rho \varrho_{\mathbf{h}} \varrho_{\mathbf{g}}}{\sigma_w^2} = 1$. Furthermore, the Rician factor is $\kappa_{\mathbf{h}} = \kappa_{\mathbf{g}} = -10\text{dB}$, the number of BS antennas is $M = 4$ and the number of RIS elements is $N = 16$. It shows that our proposed coordinated RIS architecture outperforms the conventional single-connected and group-connected RIS architecture under any channel estimation error variance σ_e^2.

V. Conclusions

The non-diagonal coordinated RIS architecture was proposed for mitigating the channel fading in wireless communication systems. Since both the element connection pattern and the configurable impedances can be optimized in our proposed coordinated RIS architecture, it achieves a higher power gain than the single-connected RIS architecture and the group-connected RIS architecture. Furthermore, the power gain of our proposed RIS architecture tends to that of the fully-connected RIS architecture upon increasing of the number of RIS elements, while requiring considerably fewer configurable impedances.

References

[1] C. Pan, H. Ren, K. Wang, J. F. Kolb, M. Elkashlan, M. Chen, M. Di Renzo, Y. Hao, J. Wang, A. L. Swindlehurst *et al.*, "Reconfigurable intelligent surfaces for 6G systems: Principles, applications, and research directions," *IEEE Commun. Mag.*, vol. 59, no. 6, pp. 14–20, 2021.

[2] B. Zheng, C. You, W. Mei, and R. Zhang, "A survey on channel estimation and practical passive beamforming design for intelligent reflecting surface aided wireless communications," *IEEE Commun. Surv. Tutor.*, vol. 24, no. 2, pp. 1035–1071, 2022.

[3] Q. Wu and R. Zhang, "Intelligent reflecting surface enhanced wireless network via joint active and passive beamforming," *IEEE Trans. Wireless Commun.*, vol. 18, no. 11, pp. 5394–5409, 2019.

[4] L. Yang, F. Meng, J. Zhang, M. O. Hasna, and M. Di Renzo, "On the performance of RIS-assisted dual-hop UAV communication systems," *IEEE Trans. Veh. Technol.*, vol. 69, no. 9, pp. 10 385–10 390, 2020.

[5] Y. Pan, K. Wang, C. Pan, H. Zhu, and J. Wang, "Sum-rate maximization for intelligent reflecting surface assisted terahertz communications," *IEEE Trans. Veh. Technol.*, vol. 71, no. 3, pp. 3320–3325, 2022.

[6] X. Wang, Z. Fei, J. Huang, and H. Yu, "Joint waveform and discrete phase shift design for RIS-assisted integrated sensing and communication system under cramér-rao bound constraint," *IEEE Trans. Veh. Technol.*, vol. 71, no. 1, pp. 1004–1009, 2021.

[7] S. Shen, B. Clerckx, and R. Murch, "Modeling and architecture design of reconfigurable intelligent surfaces using scattering parameter network analysis," *IEEE Trans. Wireless Commun.*, vol. 21, no. 2, pp. 1229–1243, 2021.

[8] H. Li, S. Shen, and B. Clerckx, "Beyond diagonal reconfigurable intelligent surfaces: From transmitting and reflecting modes to single-, group-, and fully-connected architectures," *IEEE Trans. Wireless Commun.*, vol. 22, no. 4, pp. 2311–2324, 2022.

[9] ——, "Beyond diagonal reconfigurable intelligent surfaces: A multi-sector mode enabling highly directional full-space wireless coverage," *IEEE J. Sel. Areas Commun.*, vol. 41, no. 8, pp. 2446–2460, 2023.

[10] Q. Li, M. El-Hajjar, I. A. Hemadeh, A. Shojaeifard, A. Mourad, B. Clerckx, and L. Hanzo, "Reconfigurable intelligent surfaces relying on non-diagonal phase shift matrices," *IEEE Trans. Veh. Technol.*, vol. 71, no. 6, pp. 6367–6383, 2022.

[11] J. An, L. Wang, C. Xu, L. Gan, and L. Hanzo, "Optimal pilot power based channel estimation improves the throughput of intelligent reflective surface assisted systems," *IEEE Trans. Veh. Technol.*, vol. 69, no. 12, pp. 16 202–16 206, 2020.

[12] Q. Li, M. El-Hajjar, I. Hemadeh, A. Shojaeifard, A. A. Mourad, and L. Hanzo, "Reconfigurable intelligent surface aided amplitude-and phase-modulated downlink transmission," *IEEE Trans. Veh. Technol.*, vol. 72, no. 6, pp. 8146–8151, 2023.

[13] Q. Li, M. El-Hajjar, I. Hemadeh, D. Jagyasi, A. Shojaeifard, and L. Hanzo, "Performance analysis of active RIS-aided systems in the face of imperfect CSI and phase shift noise," *IEEE Trans. Veh. Technol.*, vol. 72, no. 6, pp. 8140–8145, 2023.

[14] T. Van Chien, H. Q. Ngo, S. Chatzinotas, M. Di Renzo, and B. Ottersten, "Reconfigurable intelligent surface-assisted cell-free massive MIMO systems over spatially-correlated channels," *IEEE Trans. Wireless Commun.*, vol. 21, no. 7, pp. 5106–5128, 2022.

[15] S. Abeywickrama, R. Zhang, Q. Wu, and C. Yuen, "Intelligent reflecting surface: Practical phase shift model and beamforming optimization," *IEEE Trans. Commun.*, vol. 68, no. 9, pp. 5849–5863, 2020.

[16] Q. T. Ngo, K. T. Phan, A. Mahmood, and W. Xiang, "DRL-based secure beamforming for hybrid-RIS aided satellite downlink communications," in *2022 IEEE International Conference on Communication, Networks and Satellite (COMNETSAT)*. IEEE, 2022, pp. 432–437.